

ORIGINAL RESEARCH ARTICLE

Antidepressants are functional antagonists at the serotonin type 3 (5-HT₃) receptor

B Eisensamer^{1,2,6}, G Rammes^{1,6}, G Gimpl³, M Shapa², U Ferrari¹, G Hapfelmeier⁴, B Bondy², C Parsons⁵, K Gilling⁵, W Ziegglängsberger¹, F Holsboer¹ and R Rupprecht^{1,2}

¹Max-Planck-Institute of Psychiatry, Munich, Germany; ²Department of Psychiatry, Ludwig-Maximilians-Universität, Munich, Germany; ³Institute of Biochemistry, Johannes-Gutenberg-Universität, Mainz, Germany; ⁴Department of Anaesthesiology, Technische Universität München, Munich, Germany; ⁵Merz & Co. GmbH, Frankfurt, Germany

Antidepressants are commonly supposed to enhance serotonergic and/or noradrenergic neurotransmission by inhibition of neurotransmitter reuptake through binding to the respective neurotransmitter transporters or through inhibition of the monoamine oxidase. Using the concentration-clamp technique and measurements of intracellular Ca²⁺, we demonstrate that different classes of antidepressants act as functional antagonists at the human 5-HT_{3A} receptor stably expressed in HEK 293 cells and at endogenous 5-HT₃ receptors of rat hippocampal neurons and N1E-115 neuroblastoma cells. The tricyclic antidepressants desipramine, imipramine, and trimipramine, the serotonin reuptake inhibitor fluoxetine, the norepinephrine reuptake inhibitor reboxetine, and the noradrenergic and specific serotonergic antidepressant mirtazapine effectively reduced the serotonin-induced Na⁺- and Ca²⁺-currents in a dose-dependent fashion. This effect was voltage-independent and, with the exception of mirtazapine, noncompetitive. Desipramine, imipramine, trimipramine, and fluoxetine also accelerated receptor desensitization. Moclobemide and carbamazepine had no effect on the serotonin-induced cation current. By analyzing analogues of desipramine and carbamazepine, we found that a basic propylamine side chain increases the antagonistic potency of tricyclic compounds, whereas it is abolished by an uncharged carboxamide group. The antagonistic effects of antidepressants at the 5-HT₃ receptor did not correlate with their effects on membrane fluidity. In conclusion, structurally different types of antidepressants modulate the function of this ligand-gated ion channel. This may represent a yet unrecognized pharmacological principle of antidepressants.

Molecular Psychiatry (2003) 8, 994–1007. doi:10.1038/sj.mp.4001314

Keywords: 5-HT₃ receptor; antidepressant drug; noncompetitive antagonism; patch-clamp; calcium signal; ligand-gated ion channel

Introduction

Inhibition of serotonin and/or noradrenaline reuptake or the inhibition of monoamine oxidase^{1,2} are mechanisms of action shared by most antidepressants. In addition, second messenger systems (cAMP), transcription factors such as the cAMP responsive element binding protein (CREB),³ the brain-derived neurotrophic factor (BDNF),³ and components of the hypothalamic–pituitary–adrenal system⁴ have been identified as targets for antidepressants. In an attempt to reduce anticholinergic side effects, a major problem with tricyclic antidepressants, more specific compounds have been developed. These include selective serotonin reuptake inhibitors, for example,

fluoxetine, selective norepinephrine reuptake inhibitors (SNARIs), for example, reboxetine, and noradrenergic and specific serotonergic antidepressants (NaSSAs) such as mirtazapine.^{1,2,5,6} Mirtazapine is an α_2 -antagonist and competitive inhibitor of serotonin type 2 (5-HT₂) and type 3 (5-HT₃) receptors.^{1,5} It is current belief that these new antidepressants, with the exception of mirtazapine, do not interact preferentially with neurotransmitter receptors. However, preliminary investigations suggested that also fluoxetine acts as a functional antagonist at 5-HT₃ receptors localized on neurons of rat nodose ganglia.⁷ More recent electrophysiological data indicated that the antagonistic effect of fluoxetine is probably conferred by a noncompetitive mechanism of action.⁸

The 5-HT₃ receptor constitutes a cation permeable ligand-gated ion channel that shares structural features with γ -aminobutyric acid type A (GABA_A), glycine, and nicotinic acetylcholine (nACh) receptors.⁹ Functional 5-HT₃ receptors exist either as homomeric 5-HT_{3A} receptors⁹ or as heteromeric 5-HT_{3AB} receptors.^{10,11} Within the central nervous

Correspondence: Dr Rainer Rupprecht, MD, Department of Psychiatry, Ludwig-Maximilians-University, Nußbaumstrasse 7, 80336 Munich, Germany.

E-mail: Rainer.Rupprecht@psy.med.uni-muenchen.de

⁶Both authors contributed equally to this work

Received 28 June 2002; revised 4 December 2002; accepted 8 December 2002

system, 5-HT₃ receptors are highly expressed in the area postrema, hippocampus, and the amygdala.^{12,13} Rapid excitatory neurotransmission mediated by 5-HT₃ receptors results in neurotransmitter release, especially of dopamine in mesolimbic pathways.¹⁴ 5-HT₃ receptor antagonists prevent emesis induced by cytostatic drugs that are commonly employed in cancer therapy.^{15–17} Moreover, based on animal models and preliminary clinical studies, it has been suggested that 5-HT₃ receptor antagonists display anxiolytic^{18,19} and atypical antipsychotic properties.^{20–22} Ligand-gated ion channels such as 5-HT_{3A} receptors²³ or GABA_A receptors^{24,25} are targets for modulation by neuroactive steroids, which is an important principle for the regulation of neuronal excitability. If such a modulation of neurotransmitter receptors is also achieved by antidepressants, this would challenge the concept of target specificity claimed so far for these drugs and might represent a not yet recognized principle of antidepressant drug action.

In the present study, we show that different classes of antidepressants act as functional noncompetitive antagonists at the human 5-HT_{3A} receptor and at endogenous 5-HT₃ receptors of rat hippocampal neurons and of mouse neuroblastoma cells (N1E-115 cells). Moreover, we delineate characteristic structural components within these molecules that are necessary for this antagonistic action.

Materials and methods

Chemicals and drugs

The following compounds were used: serotonin (5-hydroxytryptamine, 5-HT) (Sigma, Deisenhofen, Germany), desipramine (RBI, Köln, Germany), imipramine (RBI), trimipramine (RBI), fluoxetine (Tocris, Köln, Germany), reboxetine (generous gift from Pharmacia & Upjohn, Kalamazoo, MI, USA), mirtazapine (generous gift from NV Organon, BH Oss, The Netherlands), moclobemide (generous gift from Roche, Grenzach, Germany), carbamazepine (RBI), 10,11-dihydrocarbamazepine (Aldrich, Taufkirchen, Germany), 10,11-dihydro-5H-dibenz[b,f]azepine (imidobenzyl; Aldrich), 10,11-dihydro-5H-dibenzo[a,d]cyclohepten (dibenzosuberane; Aldrich). For stock solutions (10 mM), desipramine, imipramine, trimipramine, fluoxetine, and reboxetine were dissolved in aqua-bidest., all other compounds were dissolved in ethanol.

Cell culture

Human embryonic kidney cells (HEK 293 cells) stably expressing the human 5-HT_{3A} receptor (HEK-5-HT_{3A} cells)²⁶ were cultured in minimum essential medium (MEM; Gibco, Karlsruhe, Germany) supplemented with 10% fetal calf serum (FCS; Gibco), 1% glutamine, nonessential amino acids and antibiotics (Gibco) at 37°C, 5% CO₂, and 95% humidity.

For the preparation of primary hippocampal neurons, hippocampi were obtained from rat embryos

(E20–E21) and transferred to Ca²⁺- and Mg²⁺-free Hank's-buffered salt solution (HBSS; Gibco, Karlsruhe, Germany) on ice. Cells were mechanically dissociated in 0.05% DNAase/0.3% ovomucoid (Sigma, Deisenhofen, Germany) following an 8 min preincubation with 0.66% trypsin/0.1% DNAase (Sigma). The dissociated cells were then centrifuged at 18 g for 10 min, resuspended in MEM (Gibco) and plated at a density of 150 000 cells cm⁻² onto poly-DL-ornithine (Sigma)/laminin (Gibco)-precoated plastic Petri dishes (Peske, Aindling-Arnshofen, Germany). The cells were nourished with NaHCO₃/HEPES-buffered MEM supplemented with 5% FCS and 5% horse serum (Gibco) and incubated at 37°C with 5% CO₂ at 95% humidity. The medium was completely exchanged following inhibition of further glial mitosis with cytosine-β-D-arabinofuranoside (ARAC, 5 μM, Sigma) after about 5 days *in vitro*.

Mouse N1E-115 neuroblastoma cells were purchased from the European collection of cell cultures (ECACC, Salisbury, UK) and stored at -80°C until further use. The cells were plated at a density of 100 000 cells cm⁻² onto plastic Petri dishes, nourished with NaHCO₃/HEPES-buffered MEM supplemented with 15% FCS (Gibco) and incubated at 37°C with 5% CO₂ at 95% humidity. The medium was exchanged completely daily. Once every 3 days, cells were reseeded onto fresh Petri dishes following treatment with trypsin-EDTA (1% in phosphate-buffered saline, PBS), resuspension in MEM and centrifugation at 200 g for 4 min.

Preparation of purified plasma membranes

HEK-5-HT_{3A} cells were harvested, washed twice with ice-cold PBS, and resuspended in homogenization buffer (20 mM HEPES, 5 mM EDTA, pH 7.4). The suspension was thoroughly homogenized and centrifuged at 40 000 g, 4°C for 30 min. The pelleted crude membrane was resuspended in ice-cold homogenization buffer and further purified by sucrose density gradient centrifugation. For this purpose, 2 ml crude membrane preparation (approximately 10 mg protein) were layered on top of a gradient consisting of 3.5 ml of 60% (w/v) sucrose and 4 ml of 35% (w/v) sucrose prepared in homogenization buffer. After centrifugation at 11 500 g, 4°C for 90 min (SW-41 rotor) the membranes at the upper 0–35% sucrose interface were collected and washed with homogenization buffer.

Electrophysiological recordings

5-HT-induced inward Na⁺-currents were recorded from lifted HEK-5-HT_{3A} and N1E-115 cells in the whole-cell voltage-clamp configuration as described previously.²³ In brief, short pulses of 5-HT (10 μM) were applied from a double-barreled application pipette moved by a piezo translator-driven device in the absence or presence of the respective drug at the indicated concentrations. 5-HT was applied in pulses of 2 s duration every 60 s. The respective drugs were diluted with bath solution (140 mM NaCl, 2.8 mM

KCl, and 10 mM HEPES, pH 7.2) to the desired concentration. To control for any possible confounding solvent effects, cells were exposed to 0.1% ethanol in 5-HT-free or 5-HT-containing solutions. The currents were recorded at a holding potential of -50 mV (HEK-5-HT_{3A}) or -70 mV (N1E-115) with an EPC-9 amplifier (Heka, Lamprecht, Germany) and analyzed using the Heka 8.5 PulseFit and IgorPro v.4.5 (Wavemetrics, Lake Oswego, OR, USA) software on a Power Macintosh G3 computer. Only results obtained from stable responses to 5-HT which showed at least 50% recovery after removal of the drugs entered the final analysis. When the recovery was $<100\%$ both control and recovery currents were considered assuming a linear time course for the rundown of the response.

Patch-clamp recordings (-70 mV) from hippocampal neurons were made after 12–15 days *in vitro* with polished glass electrodes ($2\text{--}3\text{ M}\Omega$) in the whole cell mode at room temperature ($20\text{--}22^\circ\text{C}$) with the aid of an EPC-7 amplifier (List, World Precision Instruments, Berlin, Germany). Test substances were applied with a theta glass application system ($15\text{--}20$ ms exchange times). The contents of the intracellular solution was as follows (mM): 120 CsCl, 20 TEACl, 10 EGTA, 1 MgCl₂, 0.2 CaCl₂, 10 glucose, 2 ATP, 0.25 cAMP; pH was adjusted to 7.3 with CsOH or HCl. The extracellular solution had the following basic composition (mM): 140 NaCl, 3 KCl, 0.2 CaCl₂, 10 glucose, 10 HEPES, 4.5 sucrose, tetrodotoxin (3×10^{-4}). 5-HT₃ receptors were activated by application of $10\ \mu\text{M}$ 5-HT. Only results from stable cells were accepted for inclusion in the final analysis, that is, showing at least 50% recovery of responses to 5-HT following removal of the compounds tested.

Measurement of intracellular free calcium ion concentration ($[\text{Ca}^{2+}]_i$)

HEK-5-HT_{3A} cells were harvested and diluted with HBSS (137 mM NaCl, 5 mM KCl, 1 mM MgSO₄, 1 mM CaCl₂, 0.3 mM Na₂HPO₄, 6 mM glucose, 10 mM HEPES, pH 7.4) to 10^7 cells per ml. Cells were loaded with fura2-AM (Calbiochem, Bad Soden, Germany) at a final concentration of $3\ \mu\text{M}$ by incubation for 30 min at 37°C in the dark. This mixture was diluted 10-fold with fresh HBSS and incubated for another 10 min at room temperature in the dark. To remove external dye the sample was centrifuged (300 g , 4 min) and resuspended in fresh HBSS to yield a final cell concentration of 10^7 cells per ml. $[\text{Ca}^{2+}]_i$ was measured in cuvettes filled with $200\ \mu\text{l}$ cell suspension and $1800\ \mu\text{l}$ prewarmed HBSS (37°C) using a fluorescence spectrometer LS50 (Perkin Elmer, Überlingen, Germany). 5-HT was applied 40 s after the recording onset (total recording time 2 min). The respective drug was added into the cuvette at the indicated concentrations and preincubated for 2 min. To control for any possible confounding solvent effects, $[\text{Ca}^{2+}]_i$ was recorded at a constant ethanol concentration of 0.1% in the sample mixtures. Throughout the recording, the mixture in the cuvette was continuously stirred and kept at 37°C .

Digitonin (50 mM) and EGTA (10 mM) were used to obtain R_{max} and R_{min} .²⁷

Binding of [³H]GR65630 to membrane fractions of cells expressing the 5-HT₃ receptor

HEK-5-HT_{3A} cells of 10 confluent plates ($\varnothing 10$ cm) were harvested, washed twice with PBS, and homogenized in 6 ml of 320 mM sucrose, 50 mM Tris-HCl, 1 mM EDTA, pH 7.5. After centrifugation at 750 g for 10 min, the supernatant was recentrifuged at $100\ 000\text{ g}$ for 45 min. The resulting pellet was resuspended in 4–6 ml assay buffer (50 mM Tris-HCl, 1 mM EDTA, pH 7.5). The preparation of membrane fractions was performed at 4°C . For ligand-binding experiments, membrane fractions were incubated in microtiter plates in a total volume of $250\ \mu\text{l}$ at 37°C for 1 h with the indicated concentrations of [³H]GR65630 (75 Ci/mmol; New England Nuclear, Boston, MA, USA). Bound ligand was separated from free ligand by washing with ice-cold assay buffer and rapid filtration through Whatman GF/B filters with a Titertek cell harvester (Nunc, Wiesbaden, Germany). Radioactivity was determined by liquid scintillation spectroscopy. Nonspecific binding was determined in the presence of $10\ \mu\text{M}$ MDL 72222. Specific binding represented 80–94% of the total binding. Binding data were analyzed with the EBDA and LIGAND programs,²⁸ which provide a nonlinear, least-squares regression analysis. Data are expressed as mean \pm SD of four independent experiments.

Measurement of steady-state anisotropy

Purified plasma membranes of HEK-5-HT_{3A} cells ($50\ \mu\text{g}$ of protein each) were resuspended in buffer (5 mM Tris, pH 7.0, 25 mM NaCl) and labeled with the fluorophore 1,6-diphenyl-1,3,5-hexatriene (DPH) at a final concentration of $0.3\ \mu\text{M}$. Test substances ($10\ \mu\text{l}$ from a 100-fold stock solution) were added to 1 ml of the plasma membrane suspension, and the steady-state measurements were performed after incubation for 1 h at 30°C . For kinetic experiments, the membranes were incubated in a 1 ml cuvette at 30°C for 3–5 min until a stable baseline fluorescence was obtained. Then, test compounds ($10\ \mu\text{l}$) were added from a 100-fold stock solution, and changes in fluorescence were monitored online. The membrane suspension was mixed continuously by a magnetic stirrer. Fluorescence intensity and polarization measurements were performed in triplicate on a Quantamaster (PTI, Toronto, Canada) spectrofluorometer. The probe was excited at 362 ± 10 nm. Emission was measured at 430 ± 10 nm. A cutoff filter (GG 395) was placed in front of the emission filter to reduce light scattering. The steady-state fluorescence anisotropy, r , was determined as described previously.²⁹

Results

5-HT-induced inward-currents were recorded from human embryonic kidney cells (HEK 293 cells) stably expressing the human 5-HT_{3A} receptor. Patch-clamp

recordings were performed in the whole-cell configuration. The application of 5-HT (10 μ M) via a fast application system elicited an inward current with a time to a peak (time constant of onset, τ_{on}) of 25.8 ± 4.2 ms and a peak amplitude of 0.5–3 nA. This application induced an incomplete receptor desensitization (time constant of desensitization $\tau_{des} = 619 \pm 54$ ms). After the fast removal of 5-HT, the evoked current deactivated completely (time constant of offset $\tau_{off} = 3138 \pm 138$ ms; $n = 30$) (Figure 1a). The concomitant application of 5 μ M desipramine (DMI) markedly reduced the amplitude of the 5-HT-evoked current and accelerated its desensitization (Figure 1a; see also Figure 4a, Table 1). The inhibitory effect of DMI on this 5-HT-evoked Na⁺-current was most pronounced when DMI was present already

before 5-HT and when the DMI application outlasted the 5-HT pulse (Figure 1a, left panel). Figure 1a also depicts the antagonistic effects of DMI when DMI and 5-HT were coapplied for 2 s without pre-exposure to DMI (middle panel), and when a prolonged DMI application was interrupted by a 5-HT pulse (right panel). The inhibitory effect of DMI on the 5-HT-evoked current was voltage-independent (Figure 1b, c).

In suspensions of HEK-5-HT_{3A} cells loaded with fura2-AM application of 1 μ M 5-HT elicited an increase in [Ca²⁺]_i in a range of 50–150 nM (Figure 2a). Adding DMI decreased this 5-HT-evoked [Ca²⁺]_i increase in a dose-dependent fashion (Figure 2a). Figure 2b depicts the dose–response relation for the inhibitory effects of DMI at the 5-HT_{3A} receptor. DMI

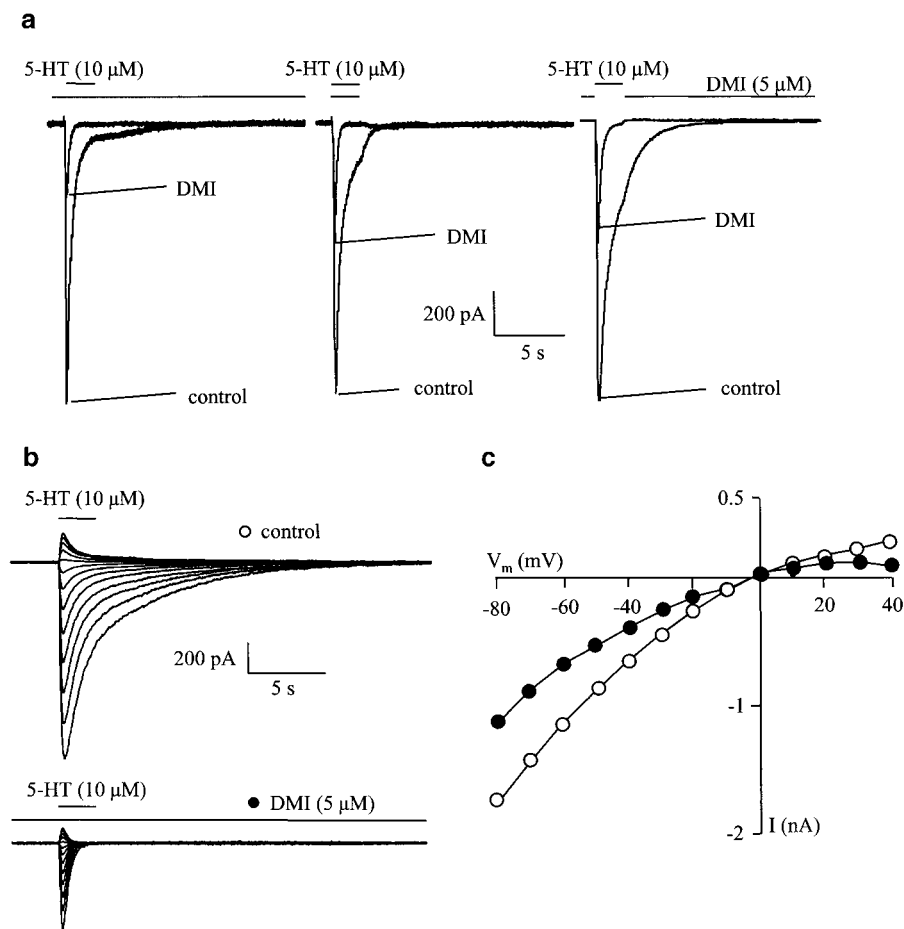


Figure 1 Effect of DMI on the 5-HT-evoked Na⁺-current through 5-HT_{3A} receptors. 5-HT-induced Na⁺-currents of HEK-5-HT_{3A} cells were recorded in the whole-cell voltage-clamp configuration. (a) Representative current traces showing different application modalities of DMI (5 μ M) and 5-HT (10 μ M). All records were obtained from the same cell. Left panel: Prolonged exposure to DMI and application pulse of 5-HT. Middle panel: Simultaneous application of 5-HT and DMI without pre-exposure to DMI. Right panel: Exposure to DMI was interrupted by application of 5-HT. The upper bar indicates the application of 10 μ M 5-HT and the lower bar the presence of 5 μ M DMI. (b) The effect of DMI on 5-HT_{3A} receptor currents is voltage-independent. Upper panel: Representative traces of the 5-HT-evoked current at different holding-potentials. The bar indicates the application of 10 μ M 5-HT. Lower panel: Representative traces of the 5-HT-evoked current after pre-exposure to 5 μ M DMI and simultaneous application of 10 μ M 5-HT and 5 μ M DMI at different holding-potentials. The upper bar indicates the application of 10 μ M 5-HT, while the lower bar indicates the presence of 5 μ M DMI. (c) Mean amplitudes of peak currents evoked by 10 μ M 5-HT in the absence (open circles) and presence (solid circles) of 5 μ M DMI are plotted against holding potential ($n = 5$).

Table 1 Effects of antidepressants on kinetics and peak amplitude of the Na⁺-current of the 5-HT_{3A} receptor

	DMI	Imipramine	Trimipramine	Fluoxetine	Reboxetine	Mirtazapine
<i>Control</i>						
τ_{on}	24.1 ± 5.3	31.7 ± 5.7	26.8 ± 3.7	21.8 ± 7.2	19.5 ± 4.5	32.0 ± 7.5
τ_{des}	569 ± 43	705 ± 59	495 ± 14	545 ± 60	551 ± 70	726 ± 72
τ_{off}	3242 ± 201	3015 ± 275	4038 ± 453	3027 ± 349	3294 ± 294	3115 ± 160
<i>With drug</i>						
τ_{on}	23.4 ± 3.9	33.9 ± 6.2	45.5 ± 3.9	11.0 ± 2.9	17.4 ± 4.3	31.9 ± 7.0
τ_{des}	255 ± 22	374 ± 49	235 ± 18	157 ± 20	484 ± 112	679 ± 75
τ_{off}	3193 ± 199	3199 ± 301	5102 ± 1235	3143 ± 316	3629 ± 422	2966 ± 260
IC ₅₀ τ_{on} (Hill coefficient)	NE	NE	2.4 ± 0.09 (0.22)	0.05 ± 0.006 (-0.17)	NE	NE
IC ₅₀ τ_{des} (Hill coefficient)	4.0 ± 0.49 (-0.44)	ND	33.1 ± 0.23 (-0.41)	0.08 ± 0.008 (-0.37)	NE	NE
IC ₅₀ τ_{off}	NE	NE	NE	NE	NE	NE
IC ₅₀ plateau (Hill coefficient)	0.17 ± 0.004 (-0.76)	0.09 ± 0.003 (-0.49)	0.26 ± 0.06 (-1.0)	0.02 ± 0.002 (-1.34)	2.38 ± 0.29 (-1.01)	0.24 ± 0.02 (-0.39)
IC ₅₀ peak (Hill coefficient)	1.09 ± 0.07 (-0.72)	1.68 ± 0.06 (-1.01)	8.3 ± 0.04 (-0.41)	2.29 ± 0.09 (-1.08)	2.66 ± 0.35 (-0.48)	0.07 ± 0.002 (-0.51)

The time constants (τ) of onset (τ_{on}), desensitization (τ_{des}) and offset (τ_{off}) kinetics measured at IC₅₀ drug concentrations of Na⁺-current indicate milliseconds (mean ± SEM; $n=7-10$). IC₅₀ values indicate micromolar concentrations; NE=no effect; ND=no dose-response relation.

concentrations within the low micromolar range markedly inhibited the 5-HT-evoked Na⁺-peak current and the 5-HT-evoked [Ca²⁺]_i peak.

The amplitude of the plateau current measured at the termination of a 2 s application of 5-HT was more effectively reduced by DMI than the peak of this inward current (Figure 2b). The dose-dependent decrease of the time constant for this desensitization suggests that DMI accelerates the desensitization of the 5-HT-evoked Na⁺-current (Figure 2c).

DMI shared this antagonistic effect at the 5-HT_{3A} receptor with imipramine and trimipramine, two other structurally related tricyclic antidepressants (Figures 3 and 4b, c), and antidepressants with different chemical structures (Figure 3) and sites of action. Fluoxetine (Figure 4d), a SSRI, reboxetine (Figure 4e), a SNARI, as well as mirtazapine (Figure 4f), a NaSSA and competitive antagonist at the 5-HT_{3A} receptor, inhibited both the 5-HT-evoked Na⁺-current and the increase in [Ca²⁺]_i in a dose-dependent fashion (Figure 5). These inhibitory effects of DMI, fluoxetine, and reboxetine on the 5-HT evoked Na⁺-current were also observed both in primary cultures of rat hippocampal neurons and in N1E-115 cells that express endogenous 5-HT₃ receptors (Figure 6, Table 2).

In contrast, no antagonistic effect at the 5-HT_{3A} receptor was found with moclobemide (Figure 4g), a selective and reversible inhibitor of the monoamine oxidase type A (MAOI-A), and carbamazepine (Figure 4h), a mood stabilizing and anticonvulsant drug. Similar to DMI (Figure 2b), imipramine, trimipramine, fluoxetine, and reboxetine exerted a more

pronounced antagonistic effect on plateau currents than on peak currents (Table 1). DMI, imipramine, trimipramine, and fluoxetine accelerated the desensitization kinetics of the 5-HT-evoked current (Figure 4a-d, right panels); fluoxetine in addition accelerated whereas trimipramine slowed down the onset kinetics (Table 1). As shown for DMI (Figure 2c), the effects of trimipramine and fluoxetine on the desensitization kinetics were dose-dependent (Table 1). In contrast to the other antidepressants, mirtazapine displayed an about three-fold higher IC₅₀ value for plateau currents than for peak currents (Table 1) in line with its competitive mode of action.

The displacement of the selective competitive 5-HT₃ receptor antagonist [³H]GR65630 was used to further characterize this antagonism. [³H]GR65630 bound with high affinity ($K_d = 1.6 \pm 0.2$ nM, $B_{max} = 2018 \pm 302$ fmol/mg protein) to membrane fractions of HEK-5-HT_{3A} cells. Only mirtazapine displaced [³H]GR65630 in a competitive manner ($K_i = 2.9 \pm 1.1$ μ M). Therefore, the antagonism of DMI, imipramine, trimipramine, fluoxetine, and reboxetine is mediated by a mechanism different from that achieved with competitive 5-HT_{3A} receptor antagonists.

Steady-state anisotropy of DPH-labeled purified plasma membranes from HEK-5-HT_{3A} cells was measured to detect eventual effects of different antidepressants on the physicochemical properties of the plasma membrane. DMI, imipramine, and fluoxetine (3–100 μ M) decreased the anisotropy of the fluorescence probe DPH within seconds in a dose-dependent fashion. At a 100 μ M concentration

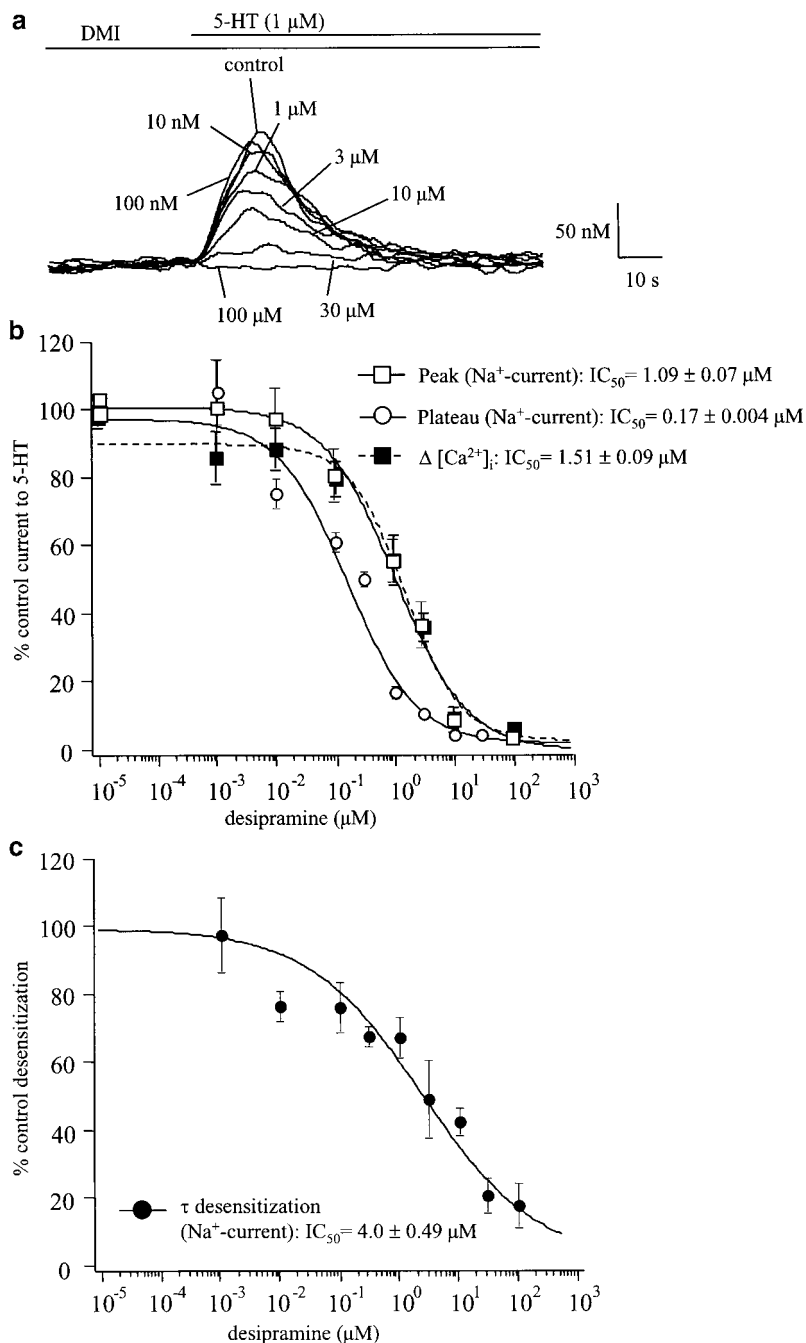


Figure 2 Dose–response relation of the effects of DMI at the 5-HT_{3A} receptor stably expressed in HEK 293 cells. (a) Functional antagonism of DMI at the 5-HT-evoked Ca²⁺-influx. Ca²⁺-influx was evaluated as an increase in the cytoplasmic free Ca²⁺-concentration ([Ca²⁺]_i) using the fluorescent dye fura-2. DMI was added to the mixture in the measuring cuvette at the indicated concentrations 2 min and 40 s prior to the stimulation of the 5-HT_{3A} receptor with 1 μ M 5-HT. The upper bar indicates the application of 1 μ M 5-HT, while the lower bar indicates the presence of DMI at the indicated concentrations. Results are shown as a representative experiment of at least four independent experiments. (b) Dose–response relation of the antagonism of DMI at peak Na⁺-currents (open squares), plateau Na⁺-currents (open circles), and [Ca²⁺]_i peak (solid squares). The plateau represents the state of the desensitized response at the end of the 2 s 5-HT-pulse. True ‘steady-state’ responses were not determined because the characteristics of the 5-HT₃ receptor desensitization did not allow this. The functional antagonism at Na⁺-currents was measured in the whole-cell configuration. DMI at the indicated concentrations was present before, during, and after the 10 μ M 5-HT-pulse. For the assessment of the functional antagonism at the 5-HT evoked [Ca²⁺]_i increase by the fura-2 method, DMI was applied at the indicated concentrations as described above. Results are expressed in percent of the amplitude obtained without DMI and represent the mean \pm SEM of four to seven independent experiments. (c) Dose–response relation of the DMI-induced decrease in the time constant of desensitization of the 5-HT-evoked Na⁺-currents. Results are expressed in percent of the desensitization time constant obtained without DMI and represent the mean \pm SEM of four to seven independent experiments. Na⁺-currents were recorded as described above.

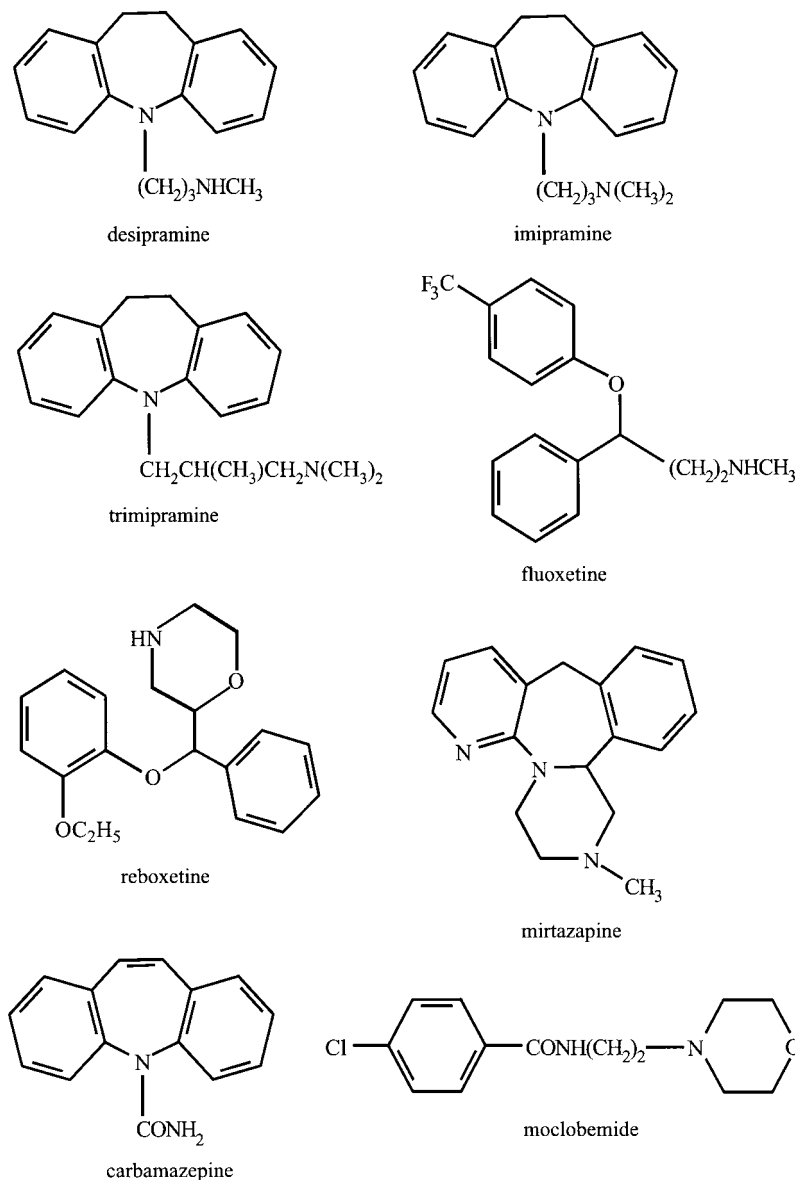


Figure 3 Molecule structure of antidepressants.

$\Delta r = -0.0113$ for DMI, -0.0069 for imipramine, and -0.0224 for fluoxetine. However, we found no correlation of the antidepressant-induced anisotropy changes and their antagonistic effect on the 5-HT-evoked inward-current (coefficient $r^2 = 0.256$). Solely fluoxetine elicited significant changes in anisotropy at concentrations less than $10 \mu\text{M}$ (eg at a $6 \mu\text{M}$ concentration $\Delta r = -0.0059$). Mirtazapine, reboxetine, moclobemide, and carbamazepine did not change anisotropy values at concentrations below $100 \mu\text{M}$ ($r = 0.223 \pm 0.009$). Only at a concentration of $100 \mu\text{M}$, mirtazapine ($\Delta r = -0.012$) and reboxetine ($\Delta r = -0.007$) caused a small decrease in anisotropy.

To identify structural components that are necessary to exert an antagonistic effect at the 5-HT_{3A} receptor, we tested the effects of various modified

tricyclic compounds on the 5-HT-evoked Na⁺-current and [Ca²⁺]_i increase (Figure 7). Like carbamazepine, 10,11-dihydrocarbamazepine had almost no inhibitory effect suggesting that the 10,11-double bond does not determine the antagonistic action on the 5-HT_{3A} receptor. Iminodibenzyl, the tricyclic core of DMI, inhibited the 5-HT-response much less than DMI (Figure 7). Apparently, the existence of an N-bound propylamine side-chain is not a prerequisite for the antagonistic effect, but it enhances antagonistic actions. However, the antagonism of tricyclic compounds at the 5-HT_{3A} receptor is abolished by an N-bound carboxamide group. To investigate whether the nitrogen atom of the middle ring affects this antagonistic action, we tested the effect of dibenzosuberane on the 5-HT-evoked responses. Interestingly, dibenzosuberane, a tricyclic compound without a nitrogen

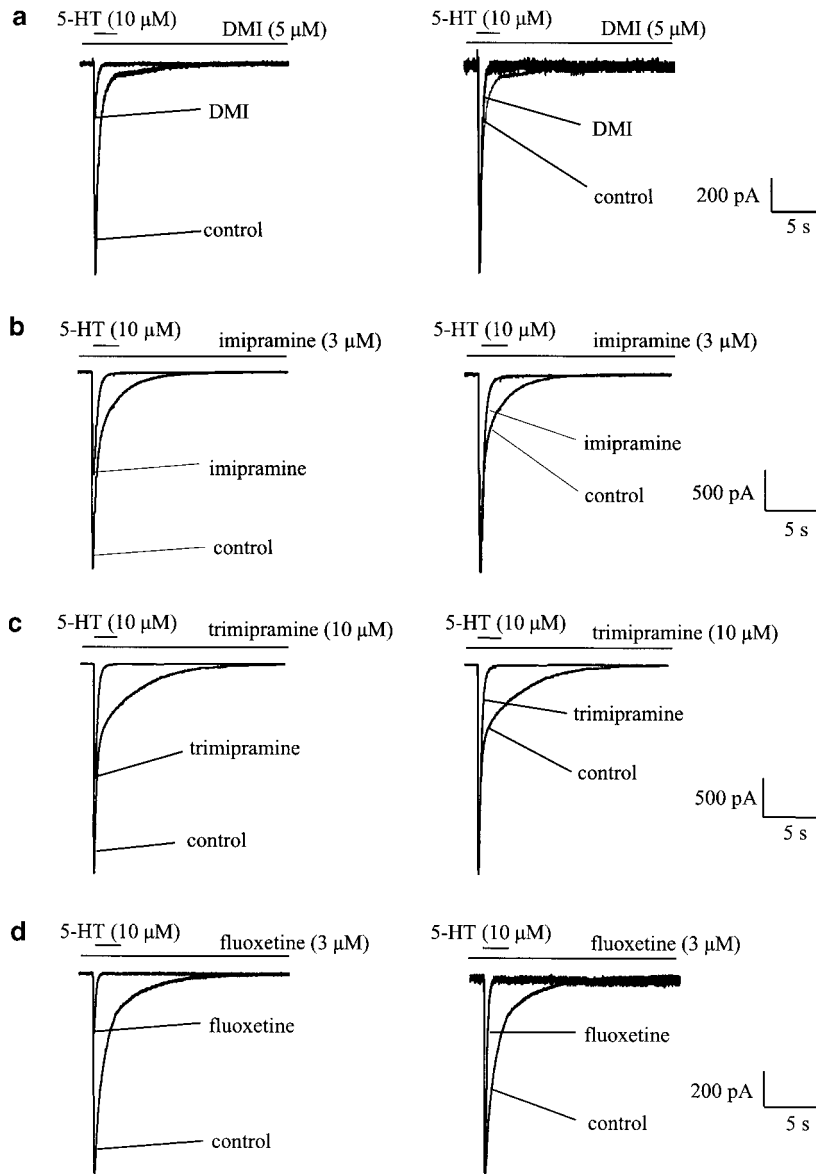


Figure 4 Effects of different types of antidepressants on the 5-HT-evoked Na⁺-current in HEK-5-HT_{3A} cells. Representative recordings of 5-HT-evoked Na⁺-currents after application of DMI (a), imipramine (b), trimipramine (c), fluoxetine (d), reboxetine (e), or mirtazapine (f) at the respective IC₅₀ concentrations (Figure 5, Table 1). Left panels represent the original traces. To delineate effects of the antidepressants on the kinetics of the 5-HT-evoked Na⁺-current, the reduced peak amplitude was adjusted to the control peak (right panel). The upper bar indicates the application of 10 μM 5-HT, while the lower bar indicates the presence of the respective antidepressant at its IC₅₀ concentration. Moclobemide (g) and carbamazepine (h) were tested at a 10 μM concentration. Peak amplitudes were not adjusted to control peaks for moclobemide and carbamazepine because these compounds did not exert inhibitory effects on the 5-HT-evoked Na⁺-current.

atom, had no effect on the Na⁺-current (Figure 7), even at a concentration of 100 μM (peak current of 110 ± 9%, mean ± SEM, *n* = 4), but it markedly reduced the 5-HT-evoked increase in [Ca²⁺]_i (Figure 7).

Discussion

The present study shows that different classes of antidepressants act as functional antagonists at the human 5-HT_{3A} receptor stably expressed in HEK 293

cells and at endogenous 5-HT₃ receptors of rat hippocampal neurons and of mouse N1E-115 neuroblastoma cells. The tricyclic antidepressants DMI, imipramine, and trimipramine, which does not mainly inhibit serotonin or norepinephrine reuptake, the SSRI fluoxetine, the SNARI reboxetine, and the NaSSA mirtazapine antagonized 5-HT-evoked Na⁺- and Ca²⁺-peak currents at low micromolar concentrations (Figures 2, 5, and 6). In accordance with previous findings, mirtazapine displaced the selec-

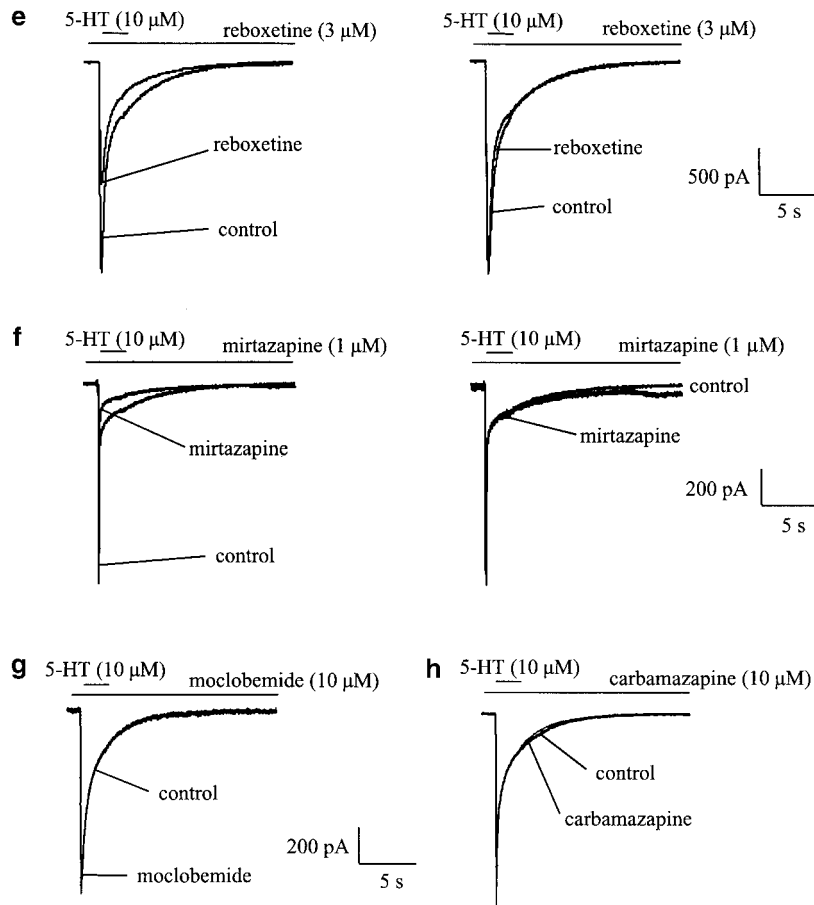


Figure 4 *Continued*

tive competitive 5-HT₃ receptor antagonist [³H]GR65630 from the 5-HT-binding site. In line with such a competitive antagonistic action, the effect of mirtazapine is mainly reflected by the reduction of the peak current. In contrast, DMI, imipramine, trimipramine, fluoxetine, and reboxetine are non-competitive antagonists with their most pronounced antagonistic effect on plateau rather than on peak currents (Table 1). The effects of DMI (Figure 1b), imipramine, trimipramine, fluoxetine, and reboxetine are voltage-independent, a finding that argues against an action as open-channel blockers at the 5-HT_{3A} receptor. This is also supported by the observation that already a pre-exposure of the receptor to these antidepressants reduced the 5-HT-evoked response (Figure 1a), indicating that they did not need to access an open-channel pore to inhibit the ion flux. A functional antagonism at the 5-HT_{3A} receptor has been reported previously for imipramine³⁰ and fluoxetine.^{7,8,30} The present study shows for the first time that these antidepressants are noncompetitive antagonists. In accordance with our results is a recent electrophysiological study that suggests that fluoxetine inhibits the 5-HT-evoked cation current in a noncompetitive manner.⁸

The noncompetitive antagonistic action of reboxetine and trimipramine differs from that observed

with the other antidepressants. Reboxetine and trimipramine apparently antagonized the 5-HT-evoked cation current by an interaction with two sites of the 5-HT_{3A} receptor reflected by a Hill coefficient near -0.5 , whereas DMI, imipramine, and fluoxetine yielded Hill coefficients of -1.08 to -1.08 , suggesting an antagonism mediated by an interaction at a single site. Reboxetine had almost no effect on the kinetics of the 5-HT-evoked currents, while DMI, imipramine, and fluoxetine markedly decreased the time constant of receptor desensitization (Figure 4a–e, Table 1), which is compatible with a noncompetitive antagonistic action.^{7,30–32} Trimipramine decreased the time constant of receptor desensitization with low potency and slowed down onset kinetics (Table 1).

In contrast to tricyclic antidepressants, fluoxetine, or reboxetine, neither the selective and reversible MAOI-A moclobemide nor the mood stabilizer and anticonvulsant carbamazepine were antagonists at the 5-HT_{3A} receptor (Figure 4g, h). This difference between the tricyclic antidepressants and carbamazepine was attributed to the characteristics of their N-bound side-chains. Our results demonstrate that the antagonistic potency increases with a basic secondary/tertiary amine, while it disappears when a polar uncharged carboxamide group is introduced (Figure 7).

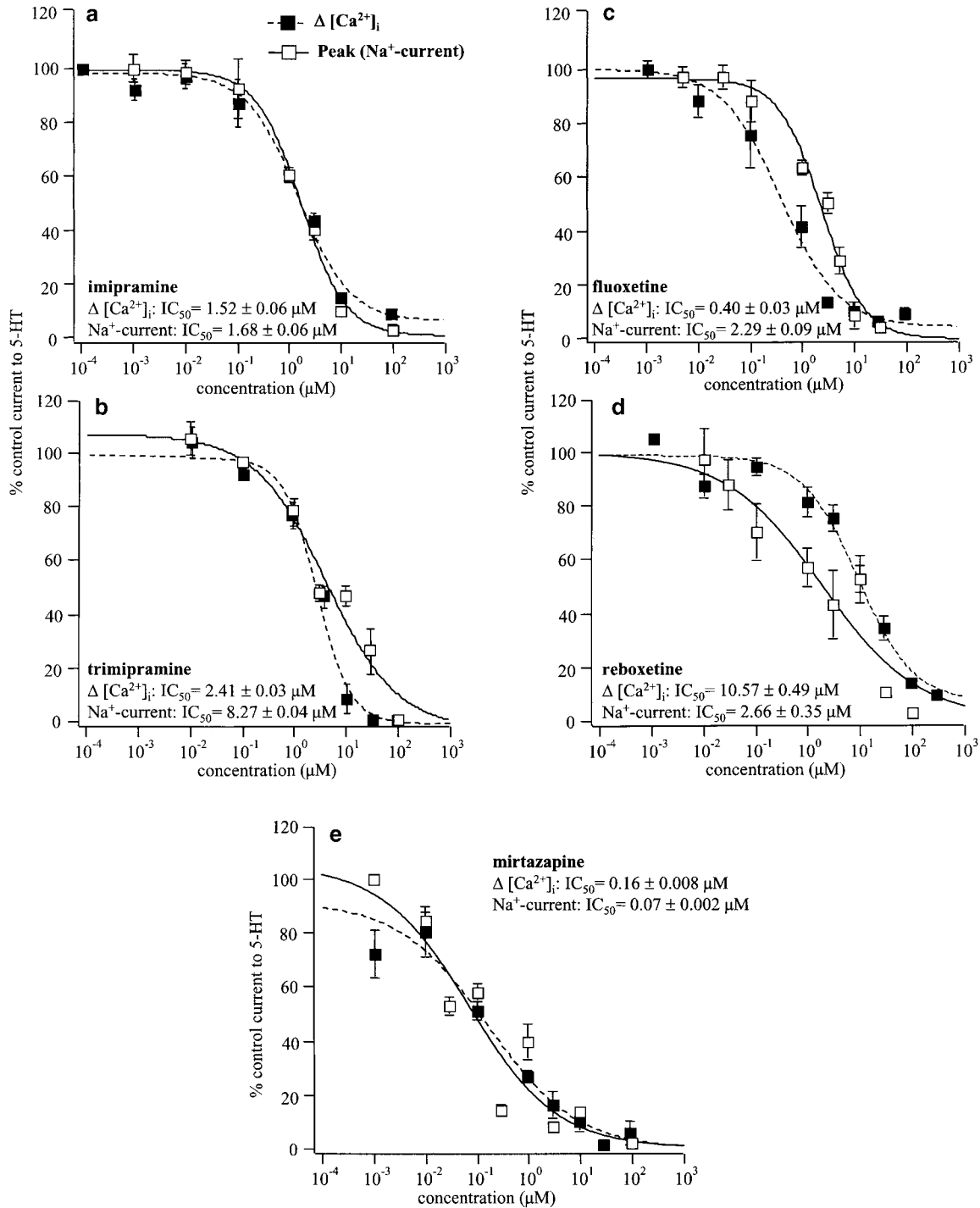


Figure 5 Dose–response relation for the functional antagonism of different types of antidepressants on the 5-HT-evoked cation current. Peak [Ca²⁺]_i (solid squares), and peak Na⁺-currents (open squares) were recorded as previously described for DMI (see legend of Figure 2b). Results are expressed in percent of the amplitude obtained without drug and represent the mean ± SEM of four to seven independent experiments.

Conclusively, the lipophilic properties of a compound not merely determine its antagonistic action at the 5-HT_{3A} receptor as it has already been shown for steroids and aromatic alcohols.²³

In the present study, we demonstrate antagonistic effects of different types of antidepressants both on

the 5-HT-evoked Na⁺-current and [Ca²⁺]_i increase in HEK-5-HT_{3A} cells. 5-HT₃ receptors are permeable for both monovalent (Na⁺, K⁺) and divalent (Ca²⁺, Mg²⁺) cations,^{10,33} with homomeric 5-HT_{3A} receptors being more Ca²⁺-permeable than heteromeric 5-HT_{3AB} receptors.¹⁰ Since Ca²⁺ is an important messenger for

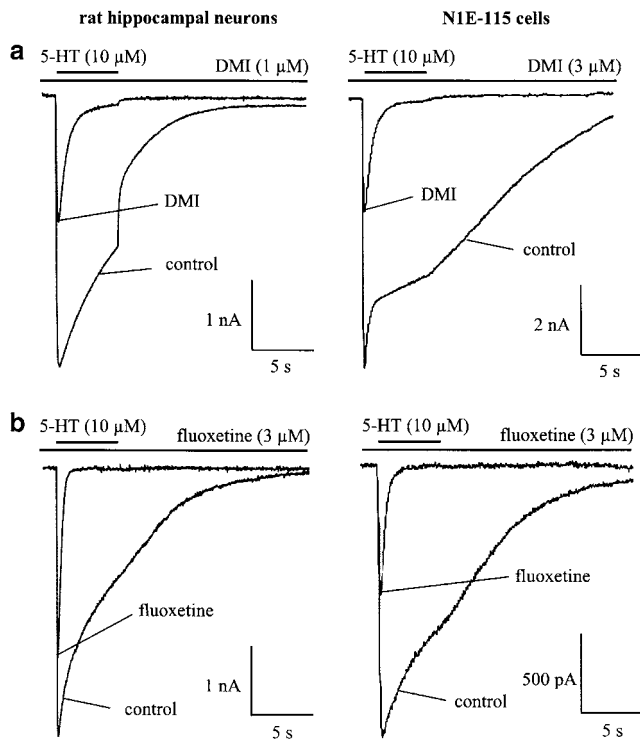


Figure 6 Effects of DMI and fluoxetine on 5-HT-evoked Na⁺-currents of endogenous 5-HT₃ receptors of rat hippocampal neurons and N1E-115 cells. Representative original traces of 5-HT-evoked Na⁺-currents after application of DMI (a) and fluoxetine (b) at the indicated concentrations. The upper bar indicates the application of 10 μM 5-HT, while the lower bar indicates the presence of the antidepressant.

neurotransmitter release and postsynaptic signaling, the reduction of Ca²⁺-influx by antidepressants may be involved in their effects on neuronal activity.³⁴ HEK 293 cells lack voltage-gated Ca²⁺-channels.³⁵ Therefore, the 5-HT-evoked rise in [Ca²⁺]_i can be attributed to Ca²⁺-ions entering the cell through 5-HT_{3A} receptor channels. All antidepressants tested reduced both Na⁺- and Ca²⁺-currents, although to a different extent. Trimipramine and fluoxetine more

effectively antagonized Ca²⁺-fluxes, whereas reboxetine and mirtazapine were more effective in reducing Na⁺-currents. This differential effect on Na⁺- and Ca²⁺-currents was also observed with dibenzosuberane, a DMI analogue, which markedly antagonized the 5-HT-evoked [Ca²⁺]_i increase, but was without effect on Na⁺-currents (Figure 7). Thus, a tricyclic compound without a nitrogen atom differentially affects the permeability of the 5-HT_{3A} receptor for Na⁺- and Ca²⁺-ions.

The permeability of nACh receptors for Na⁺ and Ca²⁺ has been shown to depend on the amino-acid sequence of a distinct channel region. Homomeric assemblies of nACh₇ subunits lose their permeability for Ca²⁺, but not for Na⁺, when a glutamate residue within the channel pore is mutated to alanine.^{36,37} Within the corresponding region of the 5-HT₃ receptor, the 5-HT_{3A} subunit contains a glutamate residue, while the 5-HT_{3B} subunit has an alanine. Thus, the reduced content of anionic residues in the channel pore of the 5-HT_{3B} subunit has been assumed to be responsible for the reduced Ca²⁺-permeability of the heteromeric 5-HT_{3AB} receptor. One possible hypothesis to explain the differential effects of distinct compounds on 5-HT-evoked Na⁺- and Ca²⁺-currents may be that some functional antagonists at the 5-HT₃ receptor modify the steric orientation of anionic residues within a critical pore region of the 5-HT₃ receptor.

To address the question whether the antagonistic effects of antidepressants at the 5-HT₃ receptor are related to their action on membrane fluidity, we assessed the effects of different classes of antidepressants on steady-state DPH fluorescence anisotropy of purified plasma membranes from HEK-5-HT_{3A} cells. Tricyclic antidepressants decreased the anisotropy values of HEK-5-HT_{3A} cells in the upper micromolar range, indicating an increase in membrane fluidity, as it has been observed in different membrane preparations from rat brains.^{38,39} In addition, spin-label studies suggested an increase in membrane fluidity after a treatment with DMI and imipramine at low micromolar concentrations.⁴⁰ However, in rat synap-

Table 2 Effects of antidepressants on peak amplitude and plateau of 5-HT evoked Na⁺-currents of endogenous 5-HT₃ receptors expressed in rat hippocampal neurons and N1E-115 cells

		DMI		Fluoxetine		Reboxetine	
		1 μM	10 μM	3 μM	30 μM	3 μM	10 μM
Rat hippocampal neurons	Peak	57.61 ± 1.28	1.04 ± 0.43	70.72 ± 12.31	2.10 ± 1.11	ND	ND
	Plateau	7.89 ± 1.57	0.46 ± 0.95	-3.64 ± 3.97	-0.50 ± 2.46	ND	ND
N1E-115 cells	Peak	27.32 ± 9.23	3.65 ± 1.72	52.66 ± 2.75	1.87 ± 0.85	45.55 ± 3.75	14.80 ± 2.27
	Plateau	1.24 ± 0.21	0.75 ± 0.47	2.56 ± 0.37	-2.18 ± 1.03	15.77 ± 3.56	2.29 ± 0.32

Values (mean ± SEM; n=3–4) indicate percent of the control current; ND=not determined.

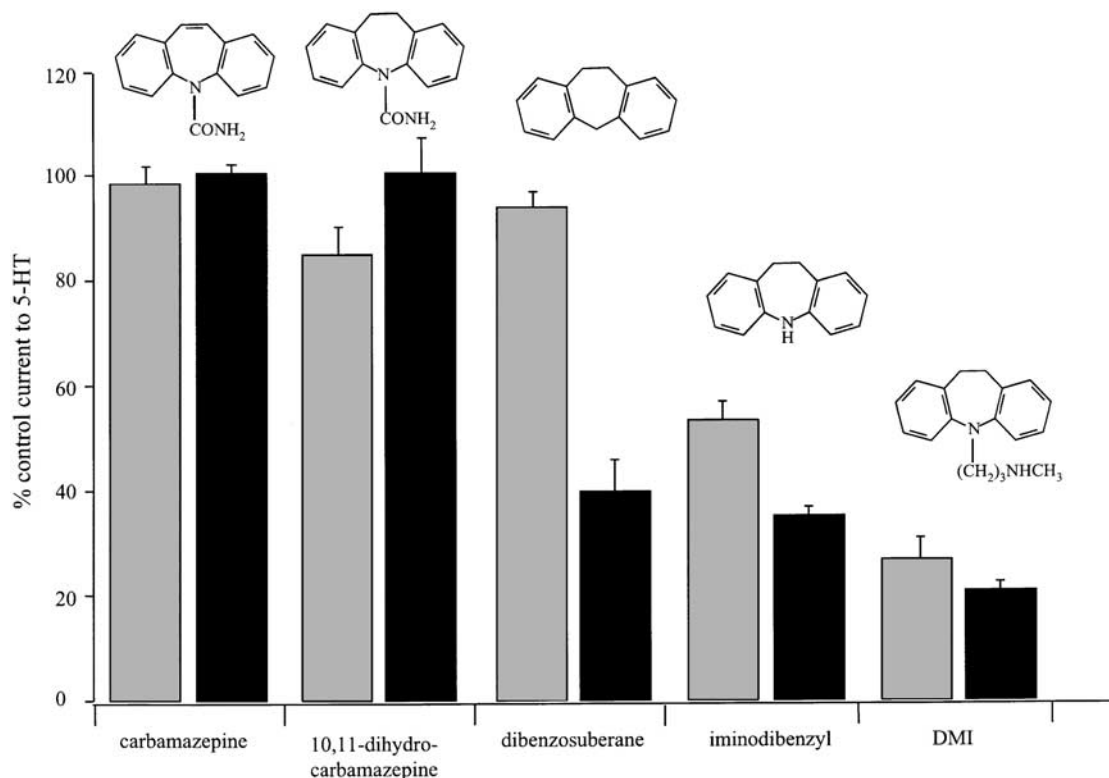


Figure 7 Antagonistic properties of carbamazepine, DMI and related tricyclic compounds at the 5-HT_{3A} receptor. Effects of tricyclic compounds (10 μ M) on the 5-HT-evoked Na⁺-peak amplitude (black rectangles) and the increase of [Ca²⁺]_i (gray rectangles) were recorded as described in the legend of Figure 2b. The Na⁺-peak amplitude evoked by 10 μ M 5-HT and the [Ca²⁺]_i increase evoked by 1 μ M 5-HT in the absence of the compounds (control) were set at 100%. Results are expressed in percent of the control measurements.

tosomal membranes, imipramine did not cause any appreciable changes in DPH fluorescence anisotropy even at concentrations up to 500 μ M.⁴¹ The present study shows that also fluoxetine, reboxetine, and mirtazapine decrease DPH fluorescence anisotropy in purified plasma membranes of HEK-5-HT_{3A} cells. However, with the exception of fluoxetine, which affected membrane anisotropy at low micromolar concentrations in a dose-dependent fashion, only concentrations far exceeding those required for a functional antagonistic effect at the 5-HT₃ receptor decreased membrane anisotropy. Moreover, there was no correlation between the effects of antidepressants on membrane anisotropy and their inhibition of the 5-HT-induced cation current. Thus, the inhibitory effects of antidepressants at this ligand-gated ion channel presumably are not merely mediated by their effects on membrane fluidity.

One hypothesis to explain the mechanisms underlying the action of noncompetitive antagonists at ligand-gated ion channels is the existence of an allosteric recognition site distinct from the agonist binding site. For the nACh receptor, photoaffinity labeling experiments revealed that steroids bind to residues located at the receptor-lipid interface and thus noncompetitively inhibit this ligand-gated ion channel.⁴² Noncompetitive inhibition of the nACh

receptor may also arise from interactions of insecticides and anesthetics with constituents of the receptor microenvironment.⁴³ Comparable investigations with 5-HT₃ receptors are lacking to date.

In conclusion, structurally different types of antidepressants are noncompetitive antagonists at the 5-HT_{3A} receptor. Since the concentrations necessary for an antagonistic action at this ligand-gated ion channel are reached both in animal studies^{44,45} and in neuroimaging studies in patients treated with fluoxetine,^{46,47} the noncompetitive modulation of ligand-gated ion channels such as the 5-HT₃ receptor challenges the concept of target specificity of new antidepressant compounds. Moreover, it may constitute a novel pharmacological principle of antidepressants.

Acknowledgements

We thank Iris Bauer, Sonja Wirth, Christiane Rewerts, Sabrina Meyr, and Sylvia de Jonge for their expert technical assistance. This work was supported by a Tandem Project of the Max-Planck-Society and the German Ministry for Education and Research within the promotional emphasis 'German Research Network on depression' (Subproject 4.3).

References

- Pacher P, Kohegyi E, Kecskemeti V, Frust S. Current trends in the development of new antidepressants. *Curr Med Chem* 2001; **8**: 89–100.
- Blakely RD. Physiological genomics of antidepressant targets: keeping the periphery in mind. *J Neurosci* 2001; **21**: 8319–8323.
- Duman RS, Heninger GR, Nestler EJ. A molecular and cellular theory of depression. *Arch Gen Psychiatry* 1997; **54**: 597–606.
- Holsboer F, Barden N. Antidepressants and hypothalamic pituitary adrenocortical regulation. *Endocrine Rev* 1996; **17**: 187–205.
- Kent JM. SNaRIs, NaSSAs, and NaRIs: new agents for the treatment of depression. *Lancet* 2000; **355**: 911–918.
- Frazer A. Serotonergic and noradrenergic reuptake inhibitors: prediction of clinical effects from *in vitro* potencies. *J Clin Psychiatry* 2001; **62**: 16–23.
- Fan P. Inhibition of a 5-HT₃ receptor-mediated current by the selective serotonin uptake inhibitor, fluoxetine. *Neurosci Lett* 1994; **173**: 210–212.
- Breitinger H-GA, Geetha N, Hess GP. Inhibition of the serotonin 5-HT₃ receptor by nicotine, cocaine, and fluoxetine investigated by rapid chemical kinetic techniques. *Biochemistry* 2001; **40**: 8419–8429.
- Maricq AV, Peterson AS, Brake AJ, Myers RM, Julius D. Primary structure and functional expression of the 5HT₃ receptor, a serotonin-gated ion channel. *Science* 1991; **254**: 432–437.
- Davies PA, Pistis M, Hanna MC, Peters JA, Lambert JJ, Hales TG et al. The 5-HT_{3B} subunit is a major determinant of serotonin-receptor function. *Nature* 1999; **397**: 359–363.
- Dubin AE, Huvar R, D'Andrea MR, Pyati J, Zju JY, Joy KC et al. The pharmacological and functional characteristics of the serotonin 5-HT₃ receptor are specifically modified by a 5-HT_{3B} receptor subunit. *J Biol Chem* 1999; **274**: 30799–30810.
- Kilpatrick GJ, Jones BJ, Tyers MB. Identification and distribution of 5-HT₃ receptor, a serotonin-gated ion channel. *Nature* 1987; **330**: 746–748.
- Tecott LH, Maricq AV, Julius D. Nervous system distribution of the 5-HT₃ receptor in rat brain using radioligand binding. *Proc Natl Acad Sci USA* 1993; **90**: 1430–1443.
- Sugita S, Shen KZ, North RA. 5-Hydroxytryptamine is a fast excitatory transmitter at 5-HT₃ receptors in rat amygdala. *Neuron* 1992; **8**: 199–203.
- Gralla RJ, Hri LMPSE, Squillant AE, Kelsen DP, Braun DW, Bordin LA et al. Antiemetic efficacy of high dose metoclopramide: randomized trials with placebo and prochlorperazine in patients with chemotherapy-induced nausea and vomiting. *N Engl J Med* 1991; **305**: 905–909.
- Kazemi-Kjellberg F, Henzi I, Tramer M. Treatment of established postoperative nausea and vomiting: a quantitative systematic review. *BMC Anesthesiol* 2001; **1**: 2.
- Ye JH, Ponnudurai R, Schaefer R. Ondansetron: a selective 5-HT₃ receptor antagonist and its applications in CNS-related disorders. *CNS Drug Rev* 2001; **7**: 199–213.
- Rodgers RJ, Cole JC, Tredwell JM. Profile of action of 5-HT₃ receptor antagonists, ondansetron and WAY 100289, in the elevated plus-maze test of anxiety of mice. *Psychopharmacology* 1995; **117**: 306–312.
- Nakagawa Y, Ishima T, Takashima T. The 5-HT₃ receptor agonist attenuates the action of antidepressants in the forced swim test in rats. *Brain Res* 1998; **786**: 189–193.
- Greenshaw AJ, Silverstone PH. The non-antiemetic uses of serotonin 5-HT₃ receptor antagonists. *Drugs* 1997; **53**: 20–39.
- Warburton AC, Cole JC, Tredwell JM. Antagonism of amphetamine-induced disruption of latent inhibition in rats by haloperidol and ondansetron: implications for a possible antipsychotic action of ondansetron. *Psychopharmacology* 1994; **114**: 657–664.
- Zoldan J, Friedberg G, Goldberg-Stern H, Melamed E. Ondansetron for hallucinosis in advanced Parkinson's disease. *Lancet* 1993; **341**: 562–563.
- Wetzel CHR, Hermann B, Behl C, Pestel E, Rammes G, Ziegler-gänsberger W et al. Functional antagonism of gonadal steroids at the 5-hydroxytryptamine type 3 receptor. *Mol Endocrinol* 1998; **12**: 1441–1451.
- Lambert JJ, Belelli D, Hill-Venning D, Peters J. Neurosteroids and GABA_A receptor function. *Trends Pharmacol Sci* 1995; **16**: 295–303.
- Rupprecht R, Holsboer F. Neuroactive steroids: mechanisms of action and neuropsychopharmacological perspectives. *Trends Neurosci* 1999; **22**: 410–416.
- Lankiewicz S, Lobitz N, Wetzel CHR, Rupprecht R, Gisselmann G, Hatt H. Molecular cloning, functional expression, and pharmacological characterization of 5-hydroxytryptamine₃ receptor cDNA and its splice variants from guinea pig. *Mol Pharmacol* 1998; **53**: 202–212.
- Bondy B, Klages U, Müller-Spahn F, Hock C. Cytosolic free [Ca²⁺] in mononuclear blood cells from demented patients and healthy controls. *Eur Arch Psychiatry Clin Neurosci* 1994; **243**: 224–228.
- Munson PJ, Rodbard D. LIGAND: a versatile computerized approach for characterization of ligand-binding systems. *Anal Biochem* 1980; **107**: 263–270.
- Gimpl G, Fahrenholz F. Human oxytocin receptors in cholesterol-rich vs. cholesterol-poor microdomains of the plasma membrane. *Eur J Biochem* 2000; **267**: 2483–2497.
- Fan P. Effects of antidepressants on the inward current mediated by 5-HT₃ receptors in rat nodose ganglion neurones. *Br J Pharmacol* 1994; **112**: 741–744.
- Bufler J, Wilhelm R, Parnas H, Franke C, Dudel J. Open channel and competitive block of the embryonic form of the nicotinic receptor of mouse myotubes by (+)-tubocurarine. *J Physiol* 1996; **495**: 83–95.
- Rammes G, Rupprecht R, Ferrari U, Ziegler-gänsberger W, Parsons CG. The N-methyl-D-aspartate receptor channel blockers memantine, MRZ 2/579 and other amino-alkyl-cyclohexanes antagonize 5-HT₃ receptor currents in cultured HEK-293 and N1E-115 cell systems in a non-competitive manner. *Neurosci Lett* 2001; **306**: 81–84.
- Brown AM, Hope AG, Lambert JJ, Peters JA. Ion permeation and conduction in a human recombinant 5-HT₃ receptor subunit (h5-HT_{3A}). *J Physiol* 1998; **507**: 653–665.
- Bliss AVP, Collingridge GL. A synaptic model of memory—long-term potentiation in the hippocampus. *Nature* 1993; **361**: 31–39.
- Hargreaves AC, Lummis SCR, Taylor CW. Ca²⁺ permeability of cloned and native 5-hydroxytryptamine type 3 receptors. *Mol Pharmacol* 1994; **46**: 1120–1128.
- Wilson GG, Karlin A. The location of the gate in the acetylcholine receptor channel. *Neuron* 1998; **20**: 1269–1281.
- Bertrand D, Galzi JL, Devillers-Thierry A, Bertrand S, Changeux JP. Mutations at two distinct sites within the channel domain M2 alter calcium permeability of neuronal A7 nicotinic receptor. *Neurobiology* 1993; **90**: 6971–6975.
- Carfagna MA, Muhoherac BB. Interaction of tricyclic drug analogs with synaptic plasma membranes: structure–mechanism relationships in inhibition of neuronal Na⁺/K⁺-ATPase activity. *Mol Pharmacol* 1993; **44**: 129–141.
- Melzacka M, Nocon H. Effect of imipramine on the membrane anisotropy and on the phospholipid methylation in the central nervous system of the rat. *J Pharm Pharmacol* 1990; **43**: 564–568.
- Lejoyeux M, Daveloose D, Mazière JC, Adès J, Viret J. A spin label study of the membrane effect of various psychoactive drugs in human erythrocytes. *Life Sci* 1992; **52**: PL-7–PL-11.
- Sanganahalli BG, Joshi PG, Joshi NB. Differential effects of tricyclic antidepressant drugs on membrane dynamics—a fluorescence spectroscopic study. *Life Sci* 2000; **68**: 81–90.
- Blanton MP, Xie Y, Dangott LJ, Cohen JB. The steroid promegestone is a noncompetitive antagonist of the *Torpedo* nicotinic acetylcholine receptor that interacts with the lipid–protein interface. *Mol Pharmacol* 1999; **55**: 269–278.
- Barrantes FJ, Antollini SS, Bouzat C, Garbus I, Massol RH. Nongenomic effects of steroids on the nicotinic acetylcholine receptor. *Kidney Int* 2000; **57**: 1382–1389.
- Weigmann H, Härtter S, Bagli M, Hiemke C. Steady state concentrations of clomipramine and its major metabolite desmethylclomipramine in rat brain and serum after oral administration of clomipramine. *Eur Neuropsychopharmacol* 2000; **10**: 401–405.

- 45 Uhr M, Steckler T, Yassouridis A, Holsboer F. Penetration of amitriptyline, but not of fluoxetine, into brain is enhanced in mice with blood–brain barrier deficiency due to Mdr1a P-glycoprotein gene disruption. *Neuropsychopharmacology* 2000; **22**: 380–387.
- 46 Bolo NR, Hodé Y, Nédélec JF, Lainé E, Wagner G, Macher JP. Brain pharmacokinetics and tissue distribution *in vivo* of fluvoxamine and fluoxetine by fluorine magnetic resonance spectroscopy. *Neuropsychopharmacology* 2000; **23**: 428–438.
- 47 Henry ME, Moore C, Kaufmann M, Michelson D, Schmidt M, Stoddard E *et al*. Brain kinetics of paroxetine and fluoxetine on the third day of placebo substitution: a fluorine MRS study. *Am J Psychiatry* 2000; **157**: 1506–1508.